Int. J. of Thermal & Environmental Engineering
Volume 19, No. 2 (2022) 93-99

Effect of Tree Shape on Micro-Climate Conditions

Mohamad Alsheikh [a], Abdelsalam Alkhalaileh [a], Isam Janajreh [a]*

[a] *Department of Mechanical Engineering, Khalifa University of Science and Technology, Abu Dhabi, UAE*

Abstract

Optimizing the microclimate conditions has become a very significant demand by public, which led to numerous research in this field. In this study, the effect of different tree shapes and their influence on the microclimate conditions will be studied using computational fluid dynamics (CFD). A baseline geometry was designed with a set of boundaries conditions and its robustness is assessed via different mesh resolutions. Three different tree shapes with the same surface area (long-triangular, short-triangular, and round) were considered and compared. The flow field is governed by the two-dimensional, steady-state, multi-species, and non-isothermal Navier-Stokes equations. In all the tree model configurations, the trees were considered the source of moisture and lower temperature than the surrounding environment. This resulted in increase in the relative humidity of the incoming ambient air and reduction in its temperature. In this analysis the incoming air was considered to follow the common power law atmospheric boundary layer ($u/U_{inf}=(y/H_o)^{1/7}$) with an inherited vertical strain rate. The presence of the trees created axial and exaggerated the vertical rate of strains. The results showed that long triangular tree shape had the biggest drop in temperatures with a value of ΔT= 4.15K (301K local value). It also resulted in a relative humidity value between 15% and 45% which is suitable for the human thermal comfort.

Keywords: *Microclimate; CFD; Human thermal comfort; Tree-shape*

1. Introduction

Since the COVID-19 outbreak, the demand for people to have their own personal private outdoor space has increased, but this space had to be also conditioned and thermally comfortable. Such demand has always been on the rise as this is the century of urbanization. An issue like this is only present in countries with hot weather throughout most of the year, a perfect example of this is the UAE. In this global warming era, this issue has become increasingly important with every decade as the weather is becoming hotter every year, this motivates researchers to find environmentally friendly methods to reduce outdoor temperature.

Vailshery et al. [1] studied the effect of street trees on the microclimate conditions and air pollution, and the study showed that the presence of street tree cover was directly connected to lowering temperature, humidity, and pollution. Wang et al. [2] conducted an experimental study on five selected cities in the Netherlands in the summer and winter. An investigation of the effects of trees on the microclimate conditions and human thermal comfort was done, and it was shown that the effect of trees on hot days was two times higher than on cold days. Another similar experimental study yielding similar results in an arid region in Algeria was also conducted by Bencheikh & Rchid [3]. Zhang et al. [4] examined the influence of vegetation on the wind environment in hot and cold seasons. Three different tree arrangements in addition to eight different species of vegetation were used, and all that has been simulated using an ENVI-met model V4. The study showed that tall trees with a large leaf area index and canopy diameter are most suitable to improve outdoor comfort. De Abreu-Harbich et al. [5] evaluated twelve different species of trees effects while focusing on the human thermal comfort, the studies also showed that the human thermal comfort can be influenced significantly and positively with the trees shading. Wang et al. [6] studied the cooling performances of trees with different crown characteristics and trunk heights, it was shown that trees with wider crowns and shorter trunks create optimal microclimate conditions in the summer. Another tree impact study was published by Mballo et al. [7], it showed a reduction of 8°C in temperatures leading to an improved human thermal comfort. To better understand the effects of other factors on the local temperature distribution and thermal comfort, Perini & Magliocco [8] conducted a study that produced excellent results towards improving micro-climate conditions. Their study was achieved by changing two significant variables which were the urban density and the height of the buildings. One concluding result asserts that the effect of vegetation is larger in areas with higher temperatures and lower relative humidity values. Another experimental study was done by Zheng et al. [9] in Guangzhou, China. This time, the characteristics of different tree species was the foundation of the study as they can lead to different cooling performances. The results showed that Ficus macrocarpa is the best cooling performer between all the eight considered species. Zölch et al. [10] work on planting trees in highly dense residential areas, stated that the strategic placement of vegetation that help cool the area down is multifold more effective than increasing the area covered with green vegetation.

* Corresponding author. Tel.: +971 2 312 3286
Fax: +9876543210; E-mail: Isam.Janajreh@ku.ac.ae

DOI: 10.5383/ijtee.19.02.006

This study is empirical evidence that the micro-scale analysis is the most efficient method to effectively choose measures to better improve micro-climate conditions.

The above literature insights one to study the effect of different tree shapes on the microclimate of the surrounding environment. Continuous monitoring of the temperature and humidity distributions will be the key to indicating the shape that will achieve the optimal conditions. Another important factor to keep an eye on is the human thermal comfort which will be considered using the Predicted-Mean-Vote model. This research complements previous studies conducted by researchers using computation fluid dynamics to study the effect of tree shapes on micro-climate conditions. In this case, three different crown shapes will be simulated with the same surface area.

2. Baseline Configuration

The baseline geometry with dimensions and the discretized mesh of the considered domain area are shown in Figure 1. A multiblock is used covering 1/7th of the domain as depicted in the figure that repeated 7 times to mesh the domain. This enabled one to use quadratic type cells and using the straightforward map meshing type. Furthermore, near the walls a propriate boundary layer is utilized at 0.5mm 1st thickness with 1.5 inflation for 10 rows. This allows accurate capturing of the dependent variables flow gradients near the ground wall and the trees. The model subjected to an incoming flow inlet (velocity and direction). The velocity profile varies according to the power law with an approximate atmospheric boundary layer height of 10 meters and $U_\infty = 2\ m/s$. At the opposite end of the inlet a symmetry is imposed meaning no axial gradients to any of the flow dependent variables. The outlet in the form of pressure and flow direction is imposed on the top of the domain while the ground is subjected to no slip & no penetration velocity. Dry air with higher temperature enters the domain. As it enters, its temperature decreases, and its relative humidity increases due to the trans-evaporative cooling phenomena that incur on the tree leave surfaces that scavenges latent heat from the incoming hot flow. This phenomenon however was not explicitly modeled but its effect. Meaning the crown tree surfaces were considered the source of humidity and at lower temperature than the influxes brought by the mean flow atmospheric boundary layer flow. That is, trees surfaces are defined to be the sources of humidity.

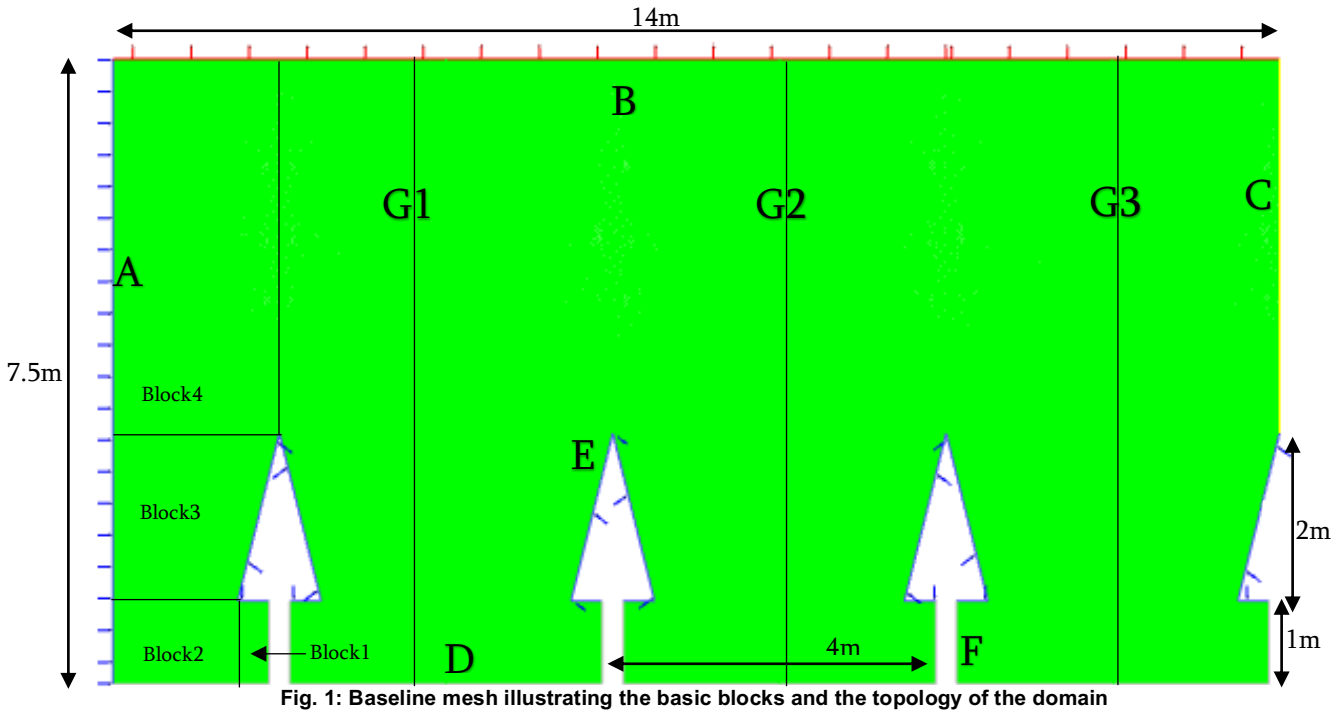

Fig. 1: Baseline mesh illustrating the basic blocks and the topology of the domain

3. Numerical Simulation

3.1. System of Equations

The flow in the system is governed by the two-dimensional-, steady-, multiple species-, and non-isothermal Navier-Stokes equations. This involves both the energy equation and the transport species for the water vapor. The statement of the mass continuity (Eq.1), the momentum (Eq.2), and the energy (Eq.8) conservation are presented as follow:

$$\text{Continuity:} \quad \frac{\partial \overline{\rho u_i}}{\partial x_i} = S_c \qquad (1)$$

Where ρ is the density, u_i is the velocity component in the x_i direction, x_i is the coordinate of the cartesian plane (i=1,2), and S_c being a mass source.

$$\text{Momentum:} \quad \frac{\partial \rho \overline{u_i u_j}}{\partial x_j} = \frac{\partial \tau_{ij}}{\partial x_j} + \overline{\rho} g_i \qquad (2)$$

Where τ_{ij} is the surface stress tensor containing viscous stress and hydrostatic pressure. ρg_i is the gravitational acceleration component in x_i direction. The constitutive equation for τ_{ij} is given as:

$$\text{Constitutive:} \quad \tau_{ij} = -\overline{p}\delta_{ij} + \mu\left(\frac{\partial \overline{\rho u_i}}{\partial x_j} + \frac{\partial \overline{\rho u_j}}{\partial x_i}\right) - \overline{\rho u_i' u_j'} \qquad (3)$$

Where μ is the dynamic viscosity, u_i' is the fluctuation of the

velocity about the velocities average. The second right hand term is the diffusion term. The full term $\overline{\rho u_i' u_j'}$ is the Reynolds stresses which utilizes the mean velocity to be modelled, it can be expressed as:

$$-\overline{\rho u_i' u_j'} = \mu_t\left(\frac{\partial \overline{\rho u_i}}{\partial x_j} + \frac{\partial \overline{\rho u_j}}{\partial x_i}\right) - \frac{2}{3}\overline{\rho} k \delta_{ij} \quad (4)$$

Where k is the turbulent kinetic energy expressed as:

$$k = \overline{u_k' u_k'} \quad (5)$$

and μ_t is the turbulent viscosity that relates to turbulent kinetic energy (k) and the dissipation turbulent rate (e) by the following equation:

$$\mu_t = f_\mu \frac{C_\mu k^2}{\varepsilon} \quad (6)$$

Where f_μ and C_μ are empirical constants. To sum the Reynolds stresses to the diffusion term, Equation (4) is substituted in equation (3) leading to an equivalent viscosity:

$$\mu_{equ} = \mu + \mu_t \quad (7)$$

The energy equation is expressed in the following form:

$$\frac{\partial}{\partial x_i}[u_i(\rho e + p)] = \frac{\partial}{\partial x_i}\left[\left(K + \frac{c_p \mu_t}{Pr_t}\right)\frac{\partial T}{\partial x_i} - \sum_j h_j J_j\right] + S_h \quad (8)$$

Where e is the total energy of the fluid with the following expression:

$$e = \sum_j h_j Y_j + u^2/2 \quad (9)$$

and K in Eq. 8 is the thermal conductivity, Cp is the constant pressure specific heat, Prt is the Prandtl number which is a ratio of kinematic turbulent viscosity over thermal diffusivity. The h is the sensible enthalpy which is defined for a j species that has the mass fraction Yj as:

$$h_j = \int_{T_{ref}}^{T} C_{p,j}\, dT \quad (10)$$

The flow has an additional specie besides the air, which is water vapor, accordingly the following transport equation is included:

$$\frac{\partial}{\partial x_i}[\rho \varphi u_i)] = \frac{\partial}{\partial x_i}\left(\Gamma \frac{\partial \varphi}{\partial x_i}\right) + S_\varphi \quad (11)$$

Where φ is any scalar property such as turbulence, k, ε, and species concentration Y. Rewriting the transport equation for the water vapor as follows:

$$\frac{\partial}{\partial x_i}[\rho Y_{H_2O} u_i)] = \frac{\partial}{\partial x_i}\left(\rho D_{H_2O} + \frac{\mu_t}{Sc_t}\right)\frac{\partial Y_{H_2O}}{\partial x_i} + S_{H_2O} \quad (12)$$

Where Sc_t and D_{H_2O} are the turbulent Schmidt number and water vapor-air diffusion coefficient, and their values are taken to be 0.7 and 2.88E-5, respectively.

3.2. Discretization and Boundary Condition

Quadrilateral mesh type is used in the baseline geometry presented in fig. 1 for discretization. To assess the robustness of the model, three levels of mesh refinements are considered in addition to the baseline. These are the fine, the coarse, and the very coarse meshes depending on the critical section that is being analyzed. This can be shown by figs. 2a through d. Two types of flow are considered: the main flow region and the flow around the trees. The geometry adapted the following thermal, species, and kinematic boundary conditions that are listed in table 1.

Table 1: Overview of baseline boundary conditions

Region	Kinematic	Thermal	Y_{H2O}	Y_{CO2}
A (Inlet)	$u/U_{inf}=(y/H)^{1/7}$	305.15K	0.001	0.0001
B (Outlet)	P=0 Atm	300K	0	0
C (Symmetry)	$u_i.n_i = 0$ $\frac{\partial \emptyset}{\partial x} = 0$	$\frac{\partial T}{\partial x} = 0$ $\frac{\partial T}{\partial y} = 0$	0	0
D&F (Wall)	No slip& penetration	298.15 K	0	0
E (Tree)	u=0.001 m/s	296.15 K	0.9	0.1

3.3. Mesh Sensitivity Study

Sensitivity analysis for the temperature and relative humidity along the horizontal line segment which stretches from 0.0 m to 14 m at 1.5 m distance from the ground was done on four levels of mesh refinements, fine, baseline, coarse I, and coarse II. The number of cells and relative error results are listed in table 2. Given the evaluated errors in the average temperature and humidity respectively as 1.54% and 2.69%, compared to 1.88% and 5.5% for the course I (and 0.89% and 7.7% for the coarse II) the baseline mesh was used for the subsequent analysis as a compromise between computational time, cost, and accuracy.

Table 2: Summary of the average temperature and their relative errors compared to the fine mesh

Mesh Resolution	Cell Count	Avg. Temp (K) & (Rel. Error)	Avg. Hum. & (Rel. Error)
Fine	1003744	298.97K	18.17%
Baseline	441588	303.58K (1.54%)	17.68% (2.69%)
Coarse I	348418	304.60K (1.88%)	19.17% (5.50%)
Coarse II	247135	301.62K (0.89%)	19.57% (7.70%)

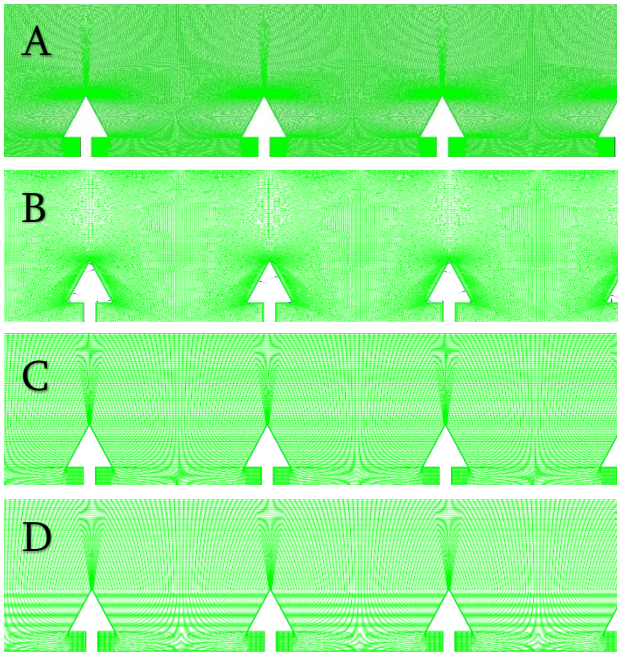

Fig. 2: Mesh refinements for the tall triangular crown trees A: fine, B: baseline, C: coarse, and D: very coarse

4. Results and discussion

The simulation model produces multiple outputs to assess the microclimate conditions and tree shape performance. However, only direct outputs that have practical implications will be taken into consideration, such as: temperature distribution contours, relative humidity contours, velocity contours, line-plots of the temperature distribution at height of 1.5 meters, and line plots of the air velocity in areas between the trees. Fig. 3 shows the temperature contours for the three shape models considered in this study. It can be observed that there is some variation in the distribution of temperature in the area around the trees for the different models. The tall triangular crown seem more diffusive than the round and the short triangular crowns. This is because the contact area between the dry air and the cool trees is the largest for this model. Since, the tall triangular crown is 2-meters tall, compared to 1-meters in the other two models. Therefore, the air flow temperature drop is the largest in this model. Such a result can be interpreted from the large coverage of the orange area that displays a temperature of 302 K.

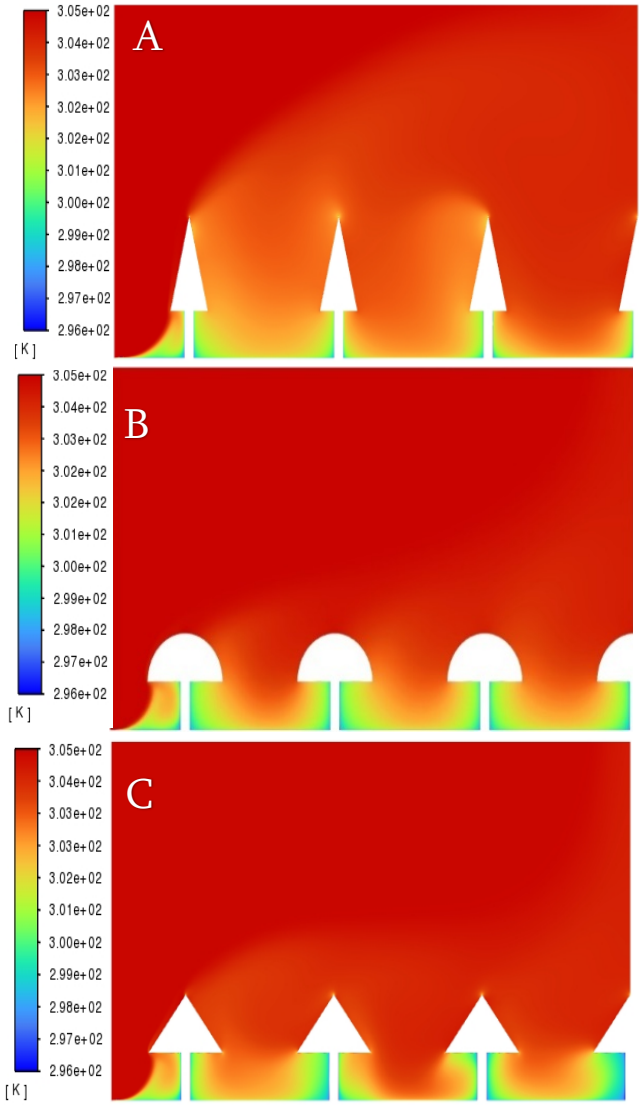

Fig. 3: Temperature distribution contours. A: tall triangular tree, B: round tree, and C: short triangular tree.

Fig. 4 depicts the relative humidity contours for the three models. In all the models, the region around the trees had a high relative humidity value which exceeded the 100%, such a phenomenon is defined as supersaturation. This occurrence is due to water vapor being found around the tree, especially on the leaves that also cause the condensation of water vapor early in the morning resulting in dew formation on the tree leaves. Here we assume the the trans-evaporation process takes place inside the tree rather on the surface which results in maintaining tree surface temperature below the incoming air inlet velocity. In our result shown in the tall triangular crown, the average relative humidity in the area is relatively low and ranging from 15% to 45%, except at the top of the tree where the supersaturation occurs. These results are well suited for the thermal human comfort as the RH levels are acceptable in the areas where humans would be residing. As for round crown tree, the relative humidity between the trees ranges from 40%-70% and the highly humid area is under the bush. Behavior similar of the round crown tree is also exhibited by the short triangular tree.

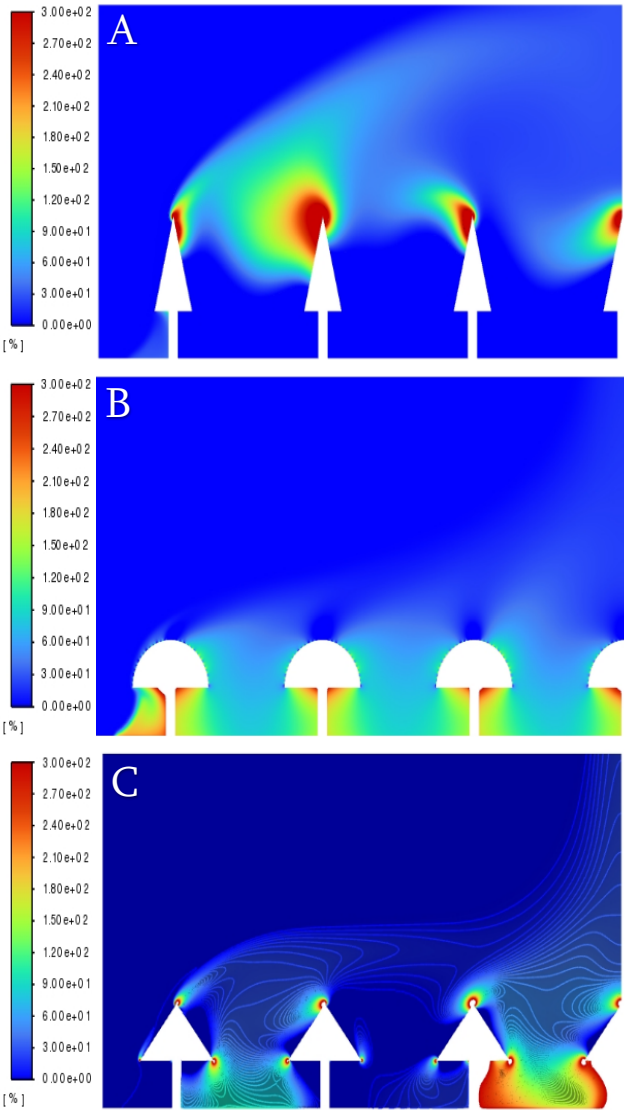

Fig. 4: Relative humidity contours. A: tall triangular tree, B: round tree, and C: short triangular tree.

The distribution of temperature and humidity is plotted at a height of 1.5 meters through the domain for the three models. This is the height taken into consideration is commonly known as the mean vote model. At this height axial distribution, the

temperature plot is presented to check the effect of the microclimate conditioning on the human thermal comfort.

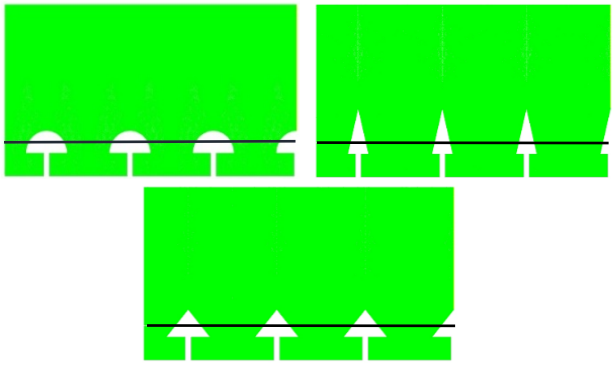

Fig. 5: 1.5-meter reference line in the models

Fig. 6 depicts line plots of the temperature at the 1.5m height which represents one of the important human thermal comfort parameters. All three models displayed a similar behavior in the region between the trees, as the air flow inlet temperature is decreased. Moreover, air flow in the tall tree crown was the lowest compared to the other models with a temperature of 302K before reaching the second tree. Also, the least thermally comfortable model in terms of temperature is the short tree crown since the lowest temperature reached was 304K, and less than a 1K drop in air flow inlet temperature.

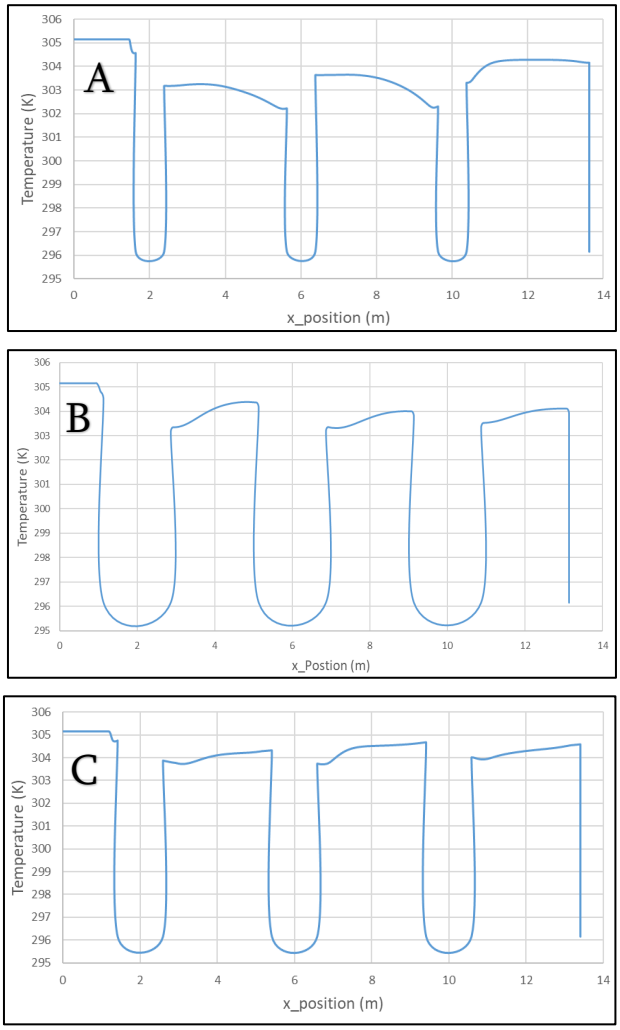

Fig. 6: Temperature values at h=1.5m, A: tall triangular tree, B: round tree, and C: short triangular tree.

Fig. 7 shows the velocity contours of the three models as it presents the pattern of the air flow inside the flow field. The velocity at the inlet follows a profile where the velocity falls in the range from 0 m/s to 5.69 m/s. It is observed in the three models that the trees act as an air canopy or blockage, since the velocity of air in the wake area behind the trees is always below 2.28 m/s. Also, in all the models the air flow reaches its maximum velocity of 5.69 m/s after encountering the first tree, where it will guide the air to flow over that area. So, in terms of the flow velocity, the area between the trees reduces the flow velocity to a range between 0.5 m/s to 2 m/s, where it is an ideal air velocity for the human thermal comfort.

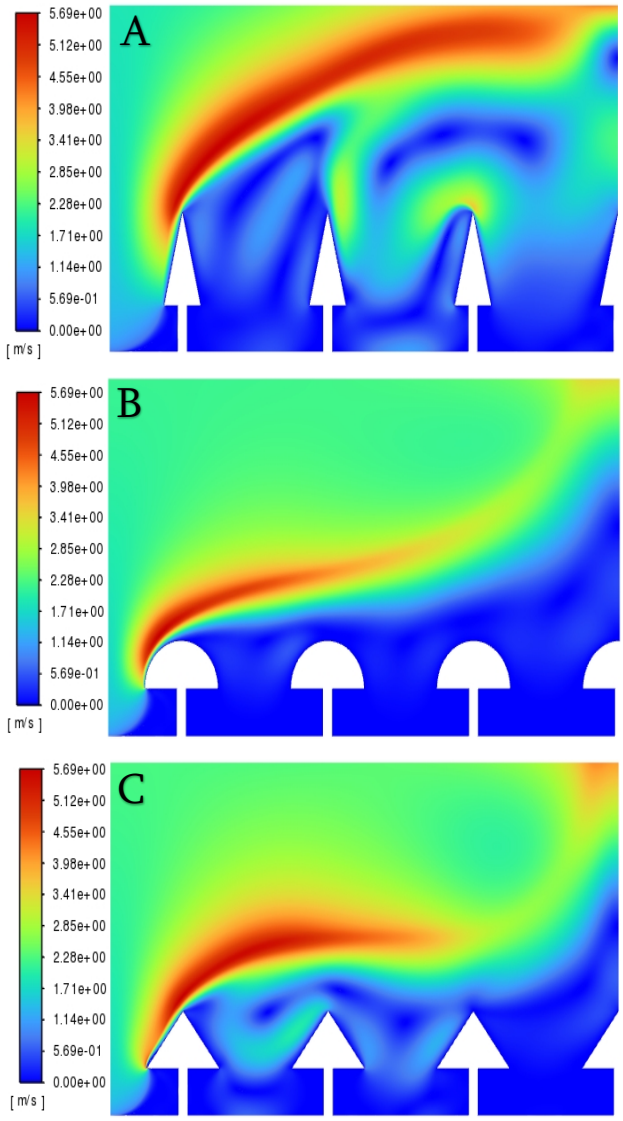

Fig. 7: Velocity contours, A: tall triangular tree, B: round tree, and C: short triangular tree.

Fig. 8 shows the air flow velocity along the height of the system for the three models. Each line represents the area between the trees in a region that is labeled in figure 1 above as G1, G2, and G3, respectively. It can be noticed that in each model, the air flow velocity at heights lower than the tree's bush is relatively lower compared to the velocities at heights above the tree's bush. Also, all models exhibit a sharp increase in the velocity above the tree since the trees act as a blockage for the air flow. In model

A this increase starts at 5 meters. However, for the round and short triangular crown models, the tree bushes are shorter leading to an earlier velocity increase from 3 meters. After that, it stabilizes at 2m/s (as the inlet velocity). Thus, according to the rate of diffusion, the rate increases with higher velocities, this will cause the air to release the contaminants and diffuses in the atmosphere and replenish it with cleaner air that is better for the human respiratory comfort. In addition, if some attention is brought to the areas where people will reside at heights of 0 to 2-meters, it can be observed that model A has an air velocity range of 0.5 m/s to 2 m/s compared to the other two models where the velocity in that region barely exceeds 0.5 m/s.

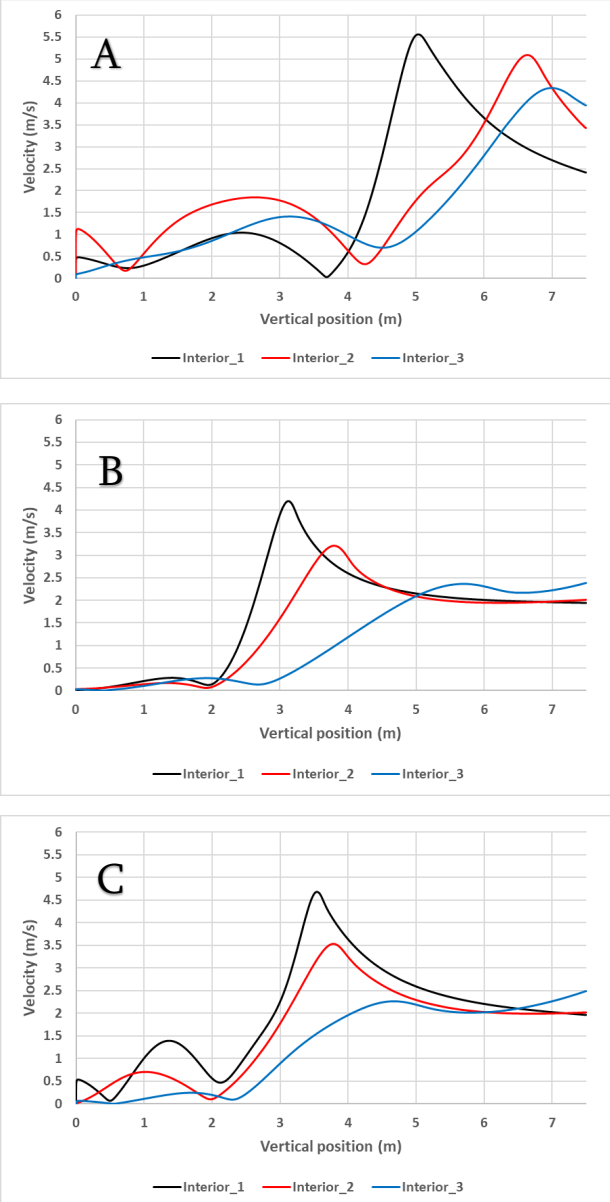

Fig. 8: Velocity magnitude along y-axis, A: tall triangular tree, B: round tree, and C: short triangular tree.

Table 3: Average values of Temperature, RH, and Velocity

Model	Temp. (K)	RH (%)	Vel. (m/s)
Tall triangular crown	303.5	17.70	0.75 m/s
Round crown	303.8	67.60	0.43 m/s
Short triangular crown	304.3	30.40	0.85 m/s

Table 3 above summarizes the average values of the temperature, RH, and velocity. These measurements were taken at height of 1.5 meters above the reference point which is the ground. As shown in the table, the highest temperature drop was in the tall triangular crown model down to a value of 303.5K. However, in the RH values, the round crown had the highest magnitude of 67.60%. This model alongside the short triangular one is close to the optimal values since magnitudes of RH higher than 70% will cause an uncomfortable and excess amount of moisture in the air [11]. Also, RH values lower than 30% will cause the air to be dry, this is also not optimal as viruses and bacteria thrive in such conditions [11]. For the air flow velocity, it ranged between 0.43 m/s to 0.85 m/s, the highest was in the short triangular tree and the lowest was in the second case. But, since they all fall in the range of the comfortable velocity range, all models are considered ideal as far as flow velocity. The short triangular crown model is still considered to be the best among them since higher velocity results in having a higher diffusion rate of harmful gases that will allow refreshing of the air faster and securing a better comfort zone.

5. Conclusions

This study was implemented to improve the fundamental understanding of the effect of the tree shapes on the micro-climate conditioning. Numerical simulation based on Navier-Stokes, steady state, turbulent, and multiple species flow was conducted. A computational fluid dynamics model has been developed based on Ansys/Fluent to solve the system. It is built on a two-dimensional, turbulent, non-isothermal and steady state flow. The inlet flow and the boundary conditions choices were selected in a range that is appropriate to UAE region. The variation of the relative humidity, temperature, and the velocity of the air flow inside the controlled area were presented and discussed. The trans-evaporation has not been explicitly considered, and the tree surfaces where assumed the source of moisture and lower temperature. The results showed that the temperature dropped in all the considered tree shapes/configurations in a range of 7°C, and the relative humidity increased and reached supersaturation situation in the region around the trees. All tree shapes reduced the air flow velocity, where that also aided in bringing the air flow velocity to a desirable range. Future research may focus on full 3D flow using 3D wedge segment for in the case of circular court yard modeling to do better justice for turbulence modeling. Furthermore, one may include tree crown mist as well CO_2 presence for explicit trans-evaporation modeling and CO_2 fate and diffusion additional to the air.

Acknowledgments

The support received from Khalifa University of Science and Technology to carry out this work is highly acknowledged.

References

1) Vailshery, Lionel Sujay, et al. “Effect of Street Trees on Microclimate and Air Pollution in a Tropical City.” Urban Forestry & Urban Greening, vol. 12,

no. 3, 2013, pp. 408–415., https://doi.org/10.1016/j.ufug.2013.03.002.

2) Wang, Y., Bakker, F., de Groot, R., Wortche, H., & Leemans, R. (2015). Effects of urban trees on local outdoor microclimate: Synthesizing field measurements by numerical modelling. Urban Ecosystems, 18(4), 1305–1331. https://doi.org/10.1007/s11252-015-0447-7
3) bencheikh, H., & Rchid, A. (2012). The effects of green spaces (Palme trees) on the microclimate in arides zones, case study: Ghardaia, Algeria. Energy Procedia, 18, 10–20. https://doi.org/10.1016/j.egypro.2012.05.013
4) Zhang, L., Zhan, Q., & Lan, Y. (2018). Effects of the tree distribution and species on outdoor environment conditions in a hot summer and cold winter zone: A case study in wuhan residential quarters. Building and Environment, 130, 27–39. https://doi.org/10.1016/j.buildenv.2017.12.014
5) de Abreu-Harbich, L. V., Labaki, L. C., & Matzarakis, A. (2015). Effect of tree planting design and tree species on human thermal comfort in the Tropics. Landscape and Urban Planning, 138, 99–109. https://doi.org/10.1016/j.landurbplan.2015.02.008
6) Wang, J., Guo, W., Wang, C., Yao, Y., Kou, K., Xian, D., & Zhang, Y. (2021). Tree crown geometry and its performances on human thermal comfort adjustment. Journal of Urban Management, 10(1), 16–26. https://doi.org/10.1016/j.jum.2021.02.001
7) Mballo, S., Herpin, S., Manteau, M., Demotes-Mainard, S., & Bournet, P. E. (2021). Impact of well-watered trees on the microclimate inside a Canyon Street scale model in outdoor environment. Urban Climate, 37, 100844. https://doi.org/10.1016/j.uclim.2021.100844
8) Perini, K., & Magliocco, A. (2014). Effects of vegetation, urban density, building height, and atmospheric conditions on local temperatures and thermal comfort. Urban Forestry & Urban Greening, 13(3), 495–506. https://doi.org/10.1016/j.ufug.2014.03.003
9) Zheng, S., Guldmann, J.-M., Liu, Z., & Zhao, L. (2018). Influence of trees on the outdoor thermal environment in subtropical areas: An experimental study in Guangzhou, China. Sustainable Cities and Society, 42, 482–497. https://doi.org/10.1016/j.scs.2018.07.025
10) Zölch, T., Maderspacher, J., Wamsler, C., & Pauleit, S. (2016). Using green infrastructure for urban climate-proofing: An evaluation of heat mitigation measures at the micro-scale. Urban Forestry & Urban Greening, 20, 305–316. https://doi.org/10.1016/j.ufug.2016.09.011
11) Feng, Z., Zhou, X., Xu, S., Ding, J., & Cao, S.-J. (2018). Impacts of humidification process on indoor thermal comfort and air quality using portable ultrasonic humidifier. *Building and Environment*, *133*, 62–72. https://doi.org/10.1016/j.buildenv.2018.02.011